NASA Technical Memorandum 100206
AIAA-87-2657

Noise of a Model High Speed Counterrotation Propeller at Simulated Takeoff/Approach Conditions (F7/A7)

Richard P. Woodward
Lewis Research Center
Cleveland, Ohio

Prepared for the
11th Aeroacoustics Conference
sponsored by the American Institute of Aeronautics and Astronautics
Sunnyvale, California, October 19-21, 1987

NASA

NOISE OF A MODEL HIGH-SPEED COUNTERROTATION PROPELLER AT SIMULATED TAKEOFF/APPROACH CONDITIONS (F7/A7)

Richard P. Woodward
National Aeronautics and Space Administration
Lewis Research Center
Cleveland, Ohio 44135

SUMMARY

A model high-speed advanced counterrotation propeller, F7/A7, was tested in the NASA Lewis Research Center's 9- by 15-Foot Anechoic Wind Tunnel at simulated takeoff/approach conditions of 0.2 Mach number. Acoustic measurements were taken with fixed floor microphones, an axially translating microphone probe, and with a "polar" microphone probe which was fixed to the propeller nacelle and could take both sideline and circumferential acoustic surveys. Aerodynamic measurements were also made to establish the propeller operating conditions. The propeller was run over a range of blade setting angles (front angle/rear angle) from 36.4°/36.5° to 41.1°/39.4°, tip speeds from 165 to 259 m/sec (540 to 850 ft/sec), rotor spacings from 1.56 to 3.63 based on forward rotor tip chord to aerodynamic separation, and angles of attack to ±16°. First order rotor alone tones showed highest directivity levels near the propeller plane, while interaction tones showed high levels throughout sideline directivity - especially toward the propeller rotation axis. Interaction tone levels were sensitive to propeller row spacing while rotor alone tones showed little spacing effect. There is a decreased noise level associated with higher propeller blade numbers for the same overall propeller thrust.

INTRODUCTION

Modern high-performance turboprop aircraft offer the promise of considerable fuel savings while still allowing for a cruise speed similar to that of current turbofan aircraft. Advanced counterrotation propellers may offer from 8 to 10 percent additional fuel savings over similar single rotation propellers at cruise conditions (ref. 1). However, there is considerable concern about the potential noise generated by such aircraft, which includes both in-flight cabin noise and community noise during takeoff and landing.

This paper presents the acoustic results for a model counterrotation propeller which was tested in the NASA Lewis 9- by 15-Foot Anechoic Wind Tunnel. The test results are for 0.20 Mach, which is representative of takeoff/approach operation. The test propeller (designated F7/A7) had 11 forward blades and nine aft blades. The propeller was tested at three rotor spacings at fixed blade angles to investigate spacing effects, and with increased blade angle at maximum spacing to investigate loading effects, and was operated over a range of rotational speeds and at angles of attack up to ±16°. Acoustic data were taken with a track "flyover" microphone probe which was fixed to the tunnel floor and with a "polar" microphone probe which was mounted on the downstream end of the propeller housing. This polar probe assembly moved with the model at angle of attack and surveyed both the angular and sideline noise field.

The unequal blade numbers of the 11 + 9 configuration of the F7/A7 propeller greatly simplified the acoustic analysis of the complicated counterrotation propeller spectra. Limited results for the 8 + 8 configuration of the F7/A7 propeller are also presented in this paper for comparison. Corresponding aerodynamic results will be presented to establish the propeller operating conditions.

APPARATUS AND PROCEDURE

The NASA Lewis 9- by 15-Foot Anechoic Wind Tunnel is located in the low-speed return leg of the supersonic 8- by 6-Foot Wind Tunnel. The maximum airflow velocity in the tunnel is slightly over 0.2 Mach, which provides a takeoff/approach test environment. The tunnel acoustic treatment was recently modified to provide anechoic conditions down to a frequency of 250 Hz, which is lower than the range of the fundamental tone produced by the F7/A7 propeller.

Acoustic instrumentation in the 9- by 15-foot tunnel consisted of fixed arrays of 0.64 cm (0.25 in.) condenser microphones on the tunnel floor, and similar microphones on two remotely-controlled acoustic survey probes. The fixed microphone array was mounted on a wooden support beam positioned 61 cm (24 in.) above the floor, and was staggered at about 10° to the tunnel flow to prevent microphone wakes from impinging on the downstream microphones. The "flyover" translating microphone probe traversed 6.50 m (21.33 ft) which covered most of the 8.2 m (27 ft) length of the treated test section. The inner microphone on this probe was located 137 m (54 in.) from the propeller axis (for 0° angle of attack), while the second microphone was located 30 cm (1 ft) ahead and 30 cm further out from the first microphone. The inner microphone of the track probe surveyed sideline angles from 18° to 150° relative to the propeller axis of rotation (at 90° referenced to the aft propeller plane) with the propeller at 0° angle of attack.

The "polar" microphone probe had the capability to survey much of the propeller noise field. As shown in the sketch of figure 2, the polar microphone probe was mounted on the downstream propeller housing and moved with the propeller at angles of attack. The probe could perform sideline acoustic surveys extending about 45° on either side of the aft propeller plane. Circumferential surveys could be made over a 240° range, being limited by support hardware interference.

The counterrotation propeller model designated F7/A7 was used in these experiments. The front propeller is nominally 62.2 cm (24.5 in.) in diameter, and the aft propeller is 60.7 cm (23.9 in.) in diameter. Most of the tests reported herein were with an 11 + 9 blade configuration; however, limited 8 + 8 results are presented for comparison. See table I for design characteristics at cruise condition of 0.72 Mach. Additional aerodynamic results for the F7/A7 8 + 8 configuration are presented in reference 2. The propeller installation in the 9- by 15 Foot Wind Tunnel was powered by two independent air turbine drives, allowing the option of independent in separating the tone content of the 8 + 8 configuration. The model was operated at propeller axis angles of attack up to ±16°.

Table II shows the propeller test conditions which are reported herein. The propeller was operated at a forward blade angle of 36.4°, aft angle of 36.5° at three blade row spacings. These spacings, measured between the blade

row pitch change axis, were 8.5 cm (3.3 in.), 10.6 cm (4.2 in.), and 15.0 cm (5.9 in.). A higher loading blade angle of 41.1°/39.4° was only tested at the maximum propeller spacing. These two blade angle configurations were tested at propeller axis angles of attack up to ±16° and at 70 to 90 percent of the design corrected rotational speed of 8371 rpm. An intermediate blade angle configuration of 39.0°/38.6° was only tested at 0° angle of attack.

There is currently some question as to which blade angles and tip speeds should be chosen to minimize noise while providing the necessary takeoff thrust. Increased blade angle with a corresponding rotational speed reduction (to maintain the same thrust) may lower the propeller noise. This could result in choosing somewhat higher takeoff blade angles than presented in this paper. However, the range of loadings and tip speeds reported are adequate to show the acoustic dependence on these parameters.

RESULTS AND DISCUSSION

All tests were performed at 0.20 tunnel Mach number. Limited aerodynamic results are presented to establish the propeller operating conditions. Acoustic results show how the propeller noise is affected by angle of attack, blade angle, tip speed, blade row spacing, and blade row numbers.

Aerodynamic performance. - Figure 3 is a propeller operating map of the total power density (based on the forward propeller), PQAT, as a function of the forward propeller advance ratio, J. PQAT is defined as:

$$\frac{\text{Power}}{(\rho)\left(\frac{\text{rev}}{\text{sec}}\right)(D^3)(\text{Annulas area})}$$

where ρ is the local air density, and D is the propeller diameter. The results in figure 3 are for the maximum blade row spacing tested. This spacing is 3.63, defined at 97 percent span as the aerodynamic inter-bladerow (i.e., t.e. to l.e.) spacing divided by the F7 aerodynamic chord. A 45° swirl angle was assumed in determining the aerodynamic spacing. Designation of the exact "takeoff design" blade angles and rotative speed is currently in a state of flux due to trade-offs between tip speed and blade loading for optimum aeroacoustic benefits The current estimate corresponds to a J value of about 0.90 and blade angles at or slightly above the maximum shown on figure 3.

Sound pressure level spectra. - The acoustic spectra for counterrotation propellers may be quite complex, consisting of both rotor-alone tone orders for each propeller and an array of interaction tones. Figure 4 presents a typical SPL spectra for the F7/A7 propeller. This spectrum, which has a bandwidth of 13 Hz, is from a fixed microphone which was located near the propeller plane. The propeller was operating at 90 percent design speed and 0° angle of attack. The forward (BPF_1) and aft (BPF_2) rotor-alone tones have the highest dB levels. Rotor-alone tones above 2BPF are essentially buried in the broadband. The interaction tones ($BPF_1 + BPF_2$, etc.) clearly dominate the spectrum at higher frequencies. Shaft order tones, based on previous experience, may be caused by blade nonuniformities based on strain gage and blade pressure instrumentation.

The spectral content at several axial locations for the same propeller operating condition is presented in figure 5. These 0 to 20 kHz spectra have a bandwidth of 50 Hz. The first order rotor-alone tones are only evident near the propeller plane (90° and 110°), while the interaction tones dominate all but the propeller plane spectra. This tendency for the interaction tones for counterrotation propellers to have high levels toward the propeller rotation axis has been well documented in the literature (refs. 3 and 4). The rotor-alone tones for counterrotation propellers behave more like those for single-rotation propellers (ref. 5), with maximum levels observed near the propeller plane and rapid noise level reduction toward the propeller axis. The following results will further explore the directivity characteristics of the counterrotating propeller. THe directivity results presented in this paper have a 16 Hz bandwidth.

Sideline directivity. - Figure 6 presents a typical sideline directivity for the F7/A7 propeller. All of the survey results in this paper are for a 16 Hz bandwidth. These results are for the "flyover" microphone probe on a 137 cm (54 in.) sideline. The rotor-alone tones (BPF_1 and BPF_2) show the expected maximum levels near the propeller plane, while the interaction tone ($BPF_1 + BPF_2$) has the highest levels toward the propeller rotation axis. Sideline directivities for interaction tones typically show minimum values near the propeller plane, as is the case for the results of figure 6. An apparent broadband noise floor at about 100 dB for this 16 Hz bandwidth analysis limited the rotor alone directivities. This broadband level is probably caused by microphone "self noise."

Figure 7 compares sideline directivities for the same propeller operating condition and circumferential location for the flyover and polar microphone probes. The polar microphone probe results were reduced by 7 dB according to the expected decay for spherical spreading. These results clearly show that the closer, 61 cm (24 in.) polar microphone probe is measuring far field results for the BPF_2 and $BPF_1 + 2BPF_2$ tones.

Rotor-alone tones are strongly affected by propeller axis angle of attack (refs. 4 and 5). This noise increase is associated with local changes in the propeller blade angle of attack, with higher blade loading producing higher noise. The maximum noise associated with propeller axis angle of attack is often observed about 90° circumferentially ahead of the maximum blade loading of the advancing propeller.

Figure 8 presents sideline directivities for the polar microphone in the aircraft flyover plane (same circumferential position as the sideline "flyover" probe). Positive angles of attack correspond to the propeller rotation axis in "climb." Figures 8(a) and (b) show the rotor-alone tone directivities. The forward rotor (BPF_1) tone varies by about 27 dB over the range of ±16° angle of attack. The aft propeller (BPF_2) tone shows more than a 20 dB variation over this angle of attack range. The directivity trends of the two representative interaction tones ($BPF_1 + Bpf_2$, and $2BPF_1 + BPF_2$) with propeller axis angle of attack are much less defined. The $BPF_1 + BPF_2$ tone (fig. 8(c)) does follow the trends of the rotor-alone tones, with maximum flyover levels for a climb condition. However, the $2BPF_1 + BPF_2$ tone (fig. 8(d)) results do not necessarily follow this trend. The acoustic response of this tone ($2BPF_1 + BPF_2$) to propeller axis angle of attack is often different from the response of other tone orders, as will be shown in subsequent figures.

Figure 9 shows the SPL in the aft propeller plane "below an aircraft" as a function of propeller axis angle of attack. These data are for the polar probe at a 61 cm (24 in.) sideline. These results, which summarize the propeller plane results of figure 8, show that the rotor alone tones are strongly affected by angle of attack. The two representative interaction tones show little dependence on angle of attack.

Circumferential directivity. - The polar microphone probe was capable of taking continuous circumferential directivities over a 240° range. Also, complete 360° circumferential directivities for operation with the propeller axis at angle of attack were produced by combining corresponding positive and negative angle of attack results. For 0° angle of attack operation the tone directivities were essentially constant over the entire angular range.

Figure 10 shows the circumferential directivity in the aft propeller plane for 16° angle of attack operation. This, and following circumferential directivity figures are oriented such that top vertical, labeled 0°, is above the aircraft. Again, a positive propeller axis angle of attack corresponds to the aircraft in a climb condition. The results of figure 10 are consistent with those for the sideline directivity at angle of attack in figure 8. The uniform circumferential directivity BPF, for zero angle of attack is shown as the dashed curve. The maximum rotor-alone tone levels are nearly below the aircraft at 180°. However, the representative interaction tone ($2BPF_1 + BPF_2$) shows a minimum below the aircraft and a maximum value slightly above the horizontal plane at about 300°. The rotor-alone tones vary circumferentially by almost 30 dB, while the interaction tone shows about a 16 dB circumferential variation.

Sixteen degrees angle of attack is a rather severe aircraft operation; however, 8° might be reasonable expected during takeoff. Figure 11 shows the circumferential directivities for the first order rotor-alone tones and the $2BPF_1 + BPF_2$ interaction tone at 8° angle of attack. Results are presented for three axial locations: downstream directivities at 124° from the propeller upstream axis, the aft propeller plane, and upstream at 60° from the propeller axis.

The relative data trends shown in figure 11 are consistent with the results of figure 10. However, the rotor-alone tones still contain considerable acoustic energy at ±30° from the aft propeller plane.

The maximum level for the aft propeller rotor-alone tone in the aft propeller plane is about 138 dB, occuring at about 210° (fig. 10(b)). This is very close to the corresponding 140 dB observed for this aft rotor-alone tone at 16° angle of attack in figure 10. This result suggests that the response of the aft rotor-alone tone to angle of attack levels out beyond 8° angle of attack.

Figure 12 shows the circumferential directivity of four interaction tones at the aft propeller plane and at the upstream position 60° from the propeller axis location. These results are also for 8° propeller axis angle of attack. Of the interaction tones presented, the $2BPF_1 + BPF_2$ tone shows the most sensitivity to angle of attack. The interaction tone levels at the forward location (fig. 12(b)) are generally slightly lower than those at the aft propeller plane.

Loading effects. - In addition to expected noise level increases with loading, it is possible that higher blade loading may affect the sensitivity of the noise directivity to angle of attack. Missing portions of the test data prevented a direct comparison of circumferential directivity with increased blade loading at the maximum blade row spacing and angle of attack.

Therefore, the following approach will be used to show the effect of blade loading on circumferential directivity at angle of attack. First, the aft rotor plane directivities at the lower blade angles (36.4°/36.5°) and 8° angle of attack will be compared for nominal and maximum rotor spacing to establish spacing effects. Next, the corresponding directivities for higher blade angles (41.1°/39.4°) still at maximum rotor spacing but at 16° angle of attack will show loading effects. This discussion will show how increased blade loading would likely produce the same sensitivity to angle of attack as was observed for ligher loading.

Figure 13 shows the circumferential tone directivity at the aft propeller plane for 8° angle of attack and maximum blade row spacing. These results are for the lower, 36.4°/36.5° blade setting angles. Figure 13 compares directly with figure 11(b), which shows the corresponding results at the nominal blade row spacing. The directivities for the rotor-alone tones are essentially the same at both blade row spacings, although the maximum tone levels (at 210°) are somewhat higher at the nominal spacing. The $2BPF_1 + BPF_2$ interaction tone directivity is about 15 dB lower near the 0° circumferential position at the maximum blade row spacing.

Figure 14 shows the circumferential tone directivity at the aft propeller plane for 16° angle of attack and maximum blade row spacing. These results are for the more highly loaded, 41.1°/39.4° blade setting angles. The results of figure 14 may be compared with the 16° angle of attack, 36.4°/36.5° blade angle results of figure 10. The rotor-alone directivities of figure 14 are essentially similar to the corresponding directivities of figure 10, indicating that blade loading does not seem to affect the rotor-alone directivities. The rotor-alone tones in figure 14 show only a small level increase with loading at $\alpha = 0°$ (see dashed curves in figs. 10 and 14) and show about the same overall sensitivity to angle of attack (about a 10 dB increase at 180°).

The 8° angle of attack spacing comparison of figures 11(b) and 13 suggested that the $2BPF_1 + BPF_2$ directivity is affected by blade row spacing. The 16° angle of attack results of figures 10 and 14 show a similar spacing effect, with the circumferential location of maximum intensity moving counter-clockwise about 130° as the blade row spacing is increased from nominal to maximum.

Aerocoustic maps. - Figure 15 shows peak tone levels measured along a 137 cm (54 in.) sideline superimposed on the propeller operating map of figure 3. Figures 15(a) and (b) are, respectively, for the forward and aft fundamental rotor-alone tones. Figure 15(c) shows the maximum sideline values for the first interaction tone, $BPF_1 + BPF_2$. These results are for 0° propeller axis angle of attack. The results of figure 15 results in an overall acoustic "picture" of the effect of the blade operating parameters on maximum tone levels.

Propeller row spacing effects. - Figure 16 shows how the fundamental rotor-alone tones and two of the interaction tones are affected by blade row spacing at 0° propeller axis angle of attack. The definition of the "spacing/

chord" parameter was explained earlier under "aerodynamic performance." The forward propeller BPF tone, which is controlled by steady loading and thickness sources, shows essentially no spacing effect. The aft propeller BPF tone shows a slight decrease with blade row spacing, which may be due to small variations in the aft propeller loading.

The interaction tones do show considerable sensitivity to blade row spacing. The $BPF_1 + BPF_2$ tone decreases by about 7 dB as the propeller row spacing increases from 1.56 to 3.63. The $2BPF_1 + BPF_2$ tone shows an even greater sensitivity with a reduction of 10 dB over this change in blade row spacing.

The circumferential directivities consistently showed constant values for the various tone orders at 0° angle of attack. Thus, the maximum sideline values of figure 16 should be representative of the noise field.

Reference 6 presents results for the 8 + 8 configuration of the F7/A7 model turboprop run in the NASA Lewis 8- by 6-Foot Wind Tunnel. The propeller was operated at high flight speed and the acoustic effect of the same blade row spacings was reported. At 0.8 tunnel Mach the first interaction tone ($BPF_1 + BPF_2$) showed an 8 dB decrease over the range of blade row spacings - essentially the same decrease as observed at 0.2 Mach in the present study. Note, that at cruise in contrast to takeoff the overall levels of the interaction tones are down compared to the rotor-alone tones. References 6 and 7 discuss how the forward rotor viscous wake and tip vortices might be expected to generate interaction tones with the downstream propeller.

Comparison of the 8 + 8 and 11 + 9 configurations. - The F7/A7 counterrotation turboprop was first run in the 8 + 8 configuration. Increasing and mismatching the blade numbers allowed for easier acoustic analysis as well as providing data on the acoustic effects of loading per blade. Figure 17 compares the sideline directivity measured by the polar microphone (61 cm (24 in.) sideline) for the two configurations at 0° angle of attack. Data are presented for two closely matched blade angle configurations with respect to total stage thrust.

Figure 17(a) compares the forward propeller BPF for the two configurations. There is a significant difference in blade number (8 and 11). The 11-blade rotor produced the higher thrust (1681 nt versus 1393 nt) at a lower blade angle (39° versus 41°). The results of 17(a) show that the eight-blade propeller was as much as 13 dB noisier at upstream angles. This relates to the higher loading per blade of the 8-blade propeller and clearly shows the acoustic advantage of increased blade number.

The aft propeller BPF, figure 17(b) is about the same for the two propellers except toward the downstream axis where the nine-blade propeller is somewhat quieter. Here the blade numbers (8 and 9), blade setting angles, and propeller thrust are more nearly matched.

The $BPF_1 + BPF_2$ interaction tone, figure 17(c) is somewhat higher for the 8 + 8 configuration on either side of the propeller plane (90°). Again, increased propeller blade numbers clearly have acoustic benefits. In this case lower loading per blade on the forward rotor decreases interaction noise.

Reference 8 presents a discussion on the acoustic effect of the number of propeller blades. This reference gives the following Gutin-type analysis for an estimate of the strength of the "m" harmonic for a propeller as

$$mBJ_{mB}(0.8M_t mB \sin \delta)$$

where m is the order of the harmonic, B is the number of blades, M_t is the blade tip rotational Mach number, and $J_n(x)$ is a Bessel function of the first kind of order n and argument x.

Solving this expression for the fundamental tone, $m = 1$, for the 8 and 11-blade forward propeller leads to an expected 6.7 dB maximum sideline noise increase for the eight-bladed propeller. Figure 17(a) shows that the maximum sideline BPF tone for the forward propeller was about 7 dB higher for the eight-bladed propeller, which is in excellent agreement with the theory of reference 8.

Solving this expression for the fundamental tone for the 8 and 9 blade aft propeller leads to an expected 2.2 dB difference in the maximum sideline noise levels for the two blade numbers. Again, this prediction is in excellent agreement with the experimental results of figure 17(b).

SUMMARY OF RESULTS

An advanced counterrotation turboprop was acoustically tested in the NASA Lewis 9- by 15-Foot Anechoic Wind Tunnel at a simulated takeoff/landing speed of 0.20 Mach. The propeller was tested over a range of blade row spacings at fixed blade angles, over a range of blade angles at maximum blade row spacing and at propeller axis angles of attack up to ±16°. Acoustic data were taken with fixed floor microphones, a translating sideline microphone, and with a unique polar microphone probe which was fixed to the downstream propeller housing, and measured both sideline and circumferential noise directivities. The following significant results were observed in this study:

1. The first order rotor-alone tones (BPF_1 and BPF_2) dominated the sideline directivities near the rotor plane. The interaction tones ($BPF_1 + BPF_2$, etc.) show high levels throughout the sideline directivities, with the highest levels often observed toward the propeller axis.

2. Sample sideline directivities for the same propeller operating conditions showed excellent agreement between the polar and translating microphone probes. This means that essentially far-field conditions exist at least down to the polar probe radius of 61 cm (24 in.), which is one propeller diameter from the propeller axis.

3. The sideline noise levels for the rotor-alone tones were strongly influenced by propeller axis angle of attack. The forward rotor BPF tone increased by about 27 dB over the range of ±16° angle of attack, while the aft rotor BPF varied by about 20 dB. The interaction tones showed a varied response to angle of attack. The $2BPF_1 + BPF_2$ tone showed the most effect, with a circumferential variation of 15 dB at 16° angle of attack. Other interaction tones showed much less sensitivity to angle of attack.

4. The circumferential directivities showed maximum rotor-alone tone levels nearly below the "aircraft" for positive (climb) angles of attack. However, the interaction tone (represented by $2BPF_1 + BPF_2$) tended to have maximum levels "above the aircraft" for the nominal blade row spacing configuration. The location of maximum interaction tone level moved circumferentially with blade row spacing.

5. The circumferential directivities associated with the 41.1°/39.4° blade angle configuration were similar to those for the more lightly-loaded 36.4°/36.5° configuration, indicating that loading-induced directivity changes are not significant over this range of blade loadings.

6. The maximum rotor-alone tone levels observed in the circumferential directivities for +8° climb were nearly as high as those observed for +16° climb. This suggests that maximum levels of propeller excitation were achieved near the +8° operating condition.

7. The interaction tones were clearly sensitive to blade row spacing, with the $2BPF_1 + BPF_2$ tone showing a 10 dB decrease as the spacing was increased from 3.6 to 1.6 spacing/rotor tip chord ratio. However, the rotor-alone tones showed little sensitivity to spacing, as expected.

8. There was a noise reduction associated with increased blade numbers (and reduced loading per blade) at constant thrust. In particular, the forward rotor BPF tone peak for the 8 + 8 configuration was about 7 dB higher than the corresponding tone peak for the 11-blade forward rotor of the 11 + 9 configuration. Likewise, the eight-blade aft rotor BPF tone was about 2 dB higher than the nine-blade aft rotor BPF tone. A Gutin-type analysis for maximum tone level as a function of blade number showed excellent agreement with these experimental results.

REFERENCES

1. Mikkelson, D.C., Mitchell, G.A., and Bober, L.J., "Summary of Recent NASA Propeller Research," Aerodynamics and Acoustics of Propellers, AGARD CP-366, 1985, pp. 12-1 to 12-24. (NASA TM-83733).

2. Sullivan, T.J., "Aerodynamic Performance of a Scale-Model, Counter-Rotating Unducted Fan, AGARD.

3. Block, P.J.W., Klatte, R.J., and Druez, P.M., "Counter-Rotating Propeller Noise Directivity and Trends," AIAA Paper 86-1927, July 1986.

4. Dittmar, J.H., "Cruise Noise of Counterrotation Propeller at Angle of Attack in Wind Tunnel," NASA TM 88869, 1986.

5. Woodward, R.P., "Measured Noise of a Scale Model High Speed Propeller at Simulated Takeoff/Approach Conditions," AIAA Paper 87-0526, Jan. 1987. (NASA TM-88920).

6. Dittmar, J.H., "The Effect of Front to Rear Propeller Spacing on the Interaction Noise of Model Counter-Rotation Propeller at Cruise Conditions," NASA TM-100121, 1987.

7. Dittmar, J.H., "Some Design Philosophy for Reducing the Community Noise of Advanced Counter-Rotation Propellers," NASA TM-87099, 1985.

8. Richards, E.J. and Mead, D.J., Noise and Acoustic Fatigue in Aeronautics, John Wiley & Sons, New York, 1968, p. 189.

TABLE I. - DESIGN CHARACTERISTICS OF F7/A7 COUNTERROTATION PROPELLER

Number of blades[a]	11/9
Design cruise Mach number	0.72
Nominal diameter, cm (in.)	62.2(24.5)/60.7(23.9)
Nominal design cruise tip speed, m/sec (ft/sec)	238(780)
Nominal design advance ratio	2.82
Hub-to-tip ratio	0.42
Geometric tip sweep, deg	34/31
Activity factor	150/150
Design power coefficient based on annulus area	4.16

[a]Front propeller/rear propeller.

TABLE II. - TEST CONDITIONS

[All data taken at 0.20 tunnel Mach.]

Blade angles	Blade row spacing	Angle of attack	Percent design speed
36.4°/36.5°	Minimum	0, ±8°, ±16°	70 ⟶ 90
36.4°/36.5°	Nominal	0, ±8°, ±16°	70 ⟶ 90
36.4°/36.5°	Maximum	0, ±8°, ±16°	70 ⟶ 90
39.0°/38.6°	Maximum	0°	70 ⟶ 90
41.1°/39.4°	Maximum	0, ±8°, ±16°	70 ⟶ 90

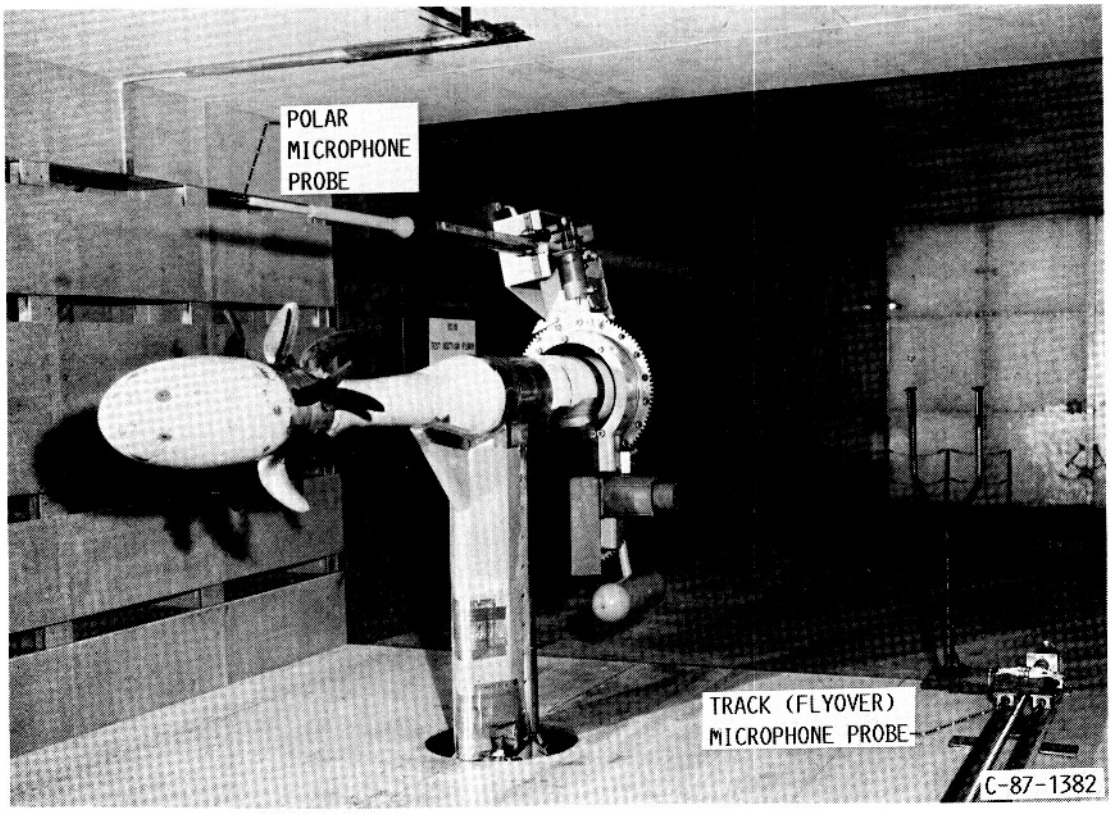

FIGURE 1. - PHOTOGRAPH OF THE UDF COUNTER-ROTATING TURBOPROP MODEL IN THE 9x15 ANECHOIC WIND TUNNEL.

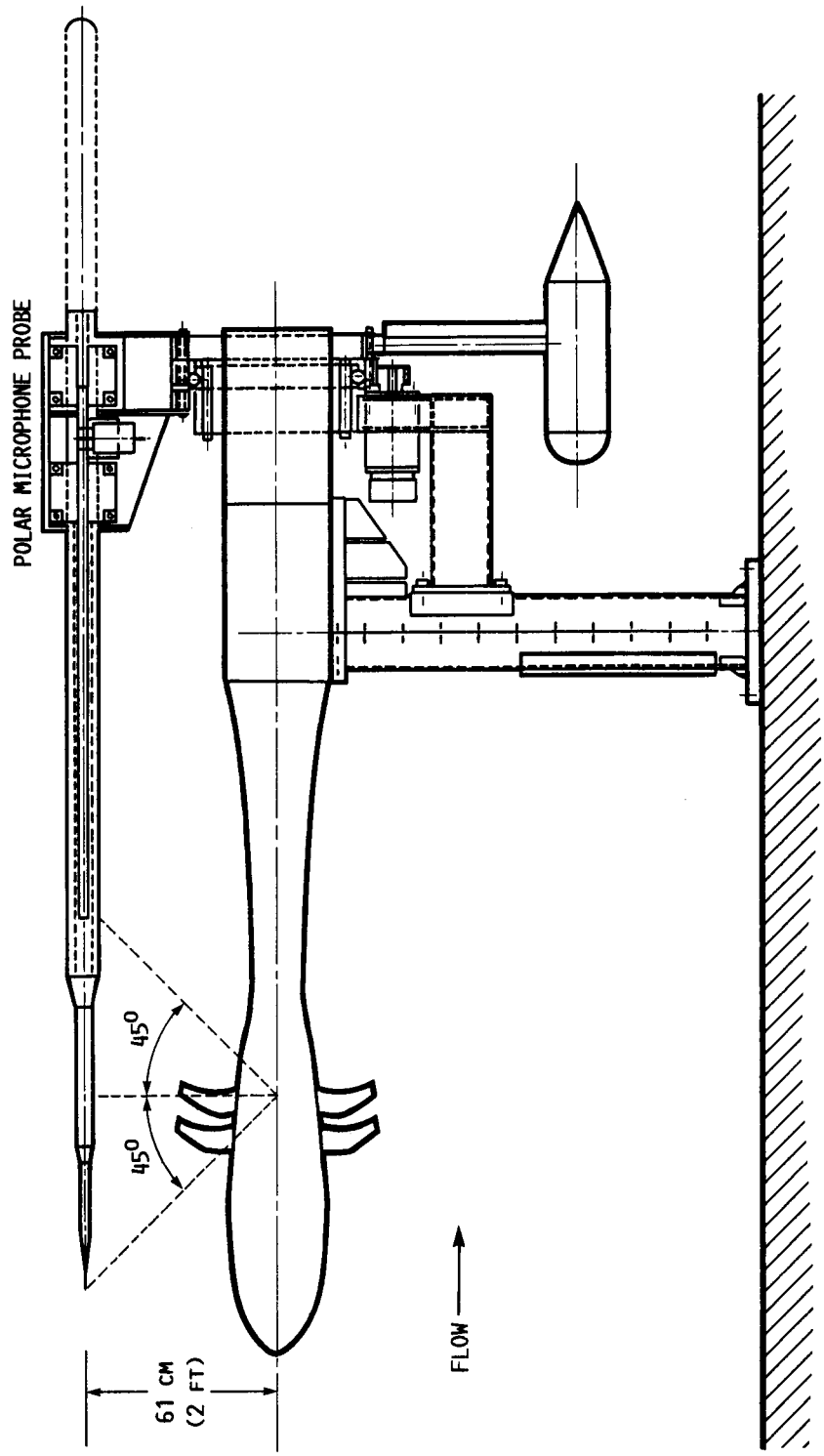

FIGURE 2. - SKETCH OF THE TURBOPROP MODEL AND POLAR MICROPHONE PROBE.

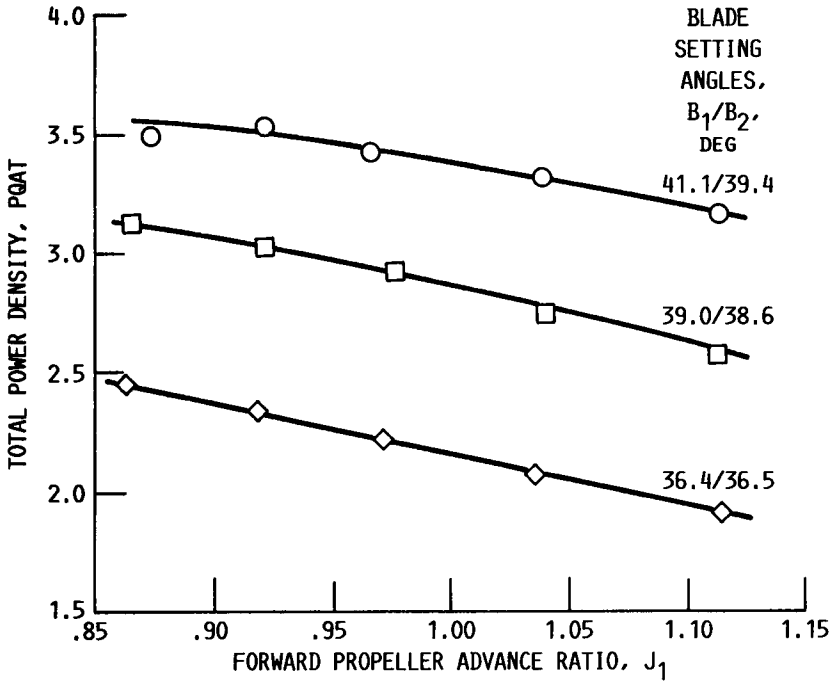

FIGURE 3. - PROPELLER OPERATING MAP FOR THREE BLADE ANGLE SETS TESTED AT 0^0 ANGLE OF ATTACK, $M_\infty = 0.2$, MAXIMUM BLADE ROW SPACING.

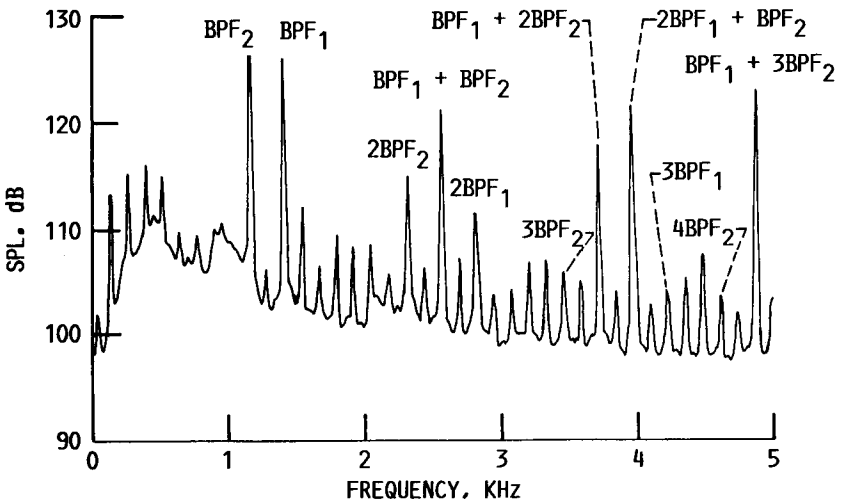

FIGURE 4. - TYPICAL SPL SPECTRUM FOR THE F7/A7 11x9 TURBOPROP. DATA IS FOR THE FIXED FLOOR MICROPHONE IN THE PROPELLER PLANE. (90 PERCENT SPD, $\alpha = 0^0$, $B = 36.4^0/36.5^0$, NOMINAL BLADE SPACING.)

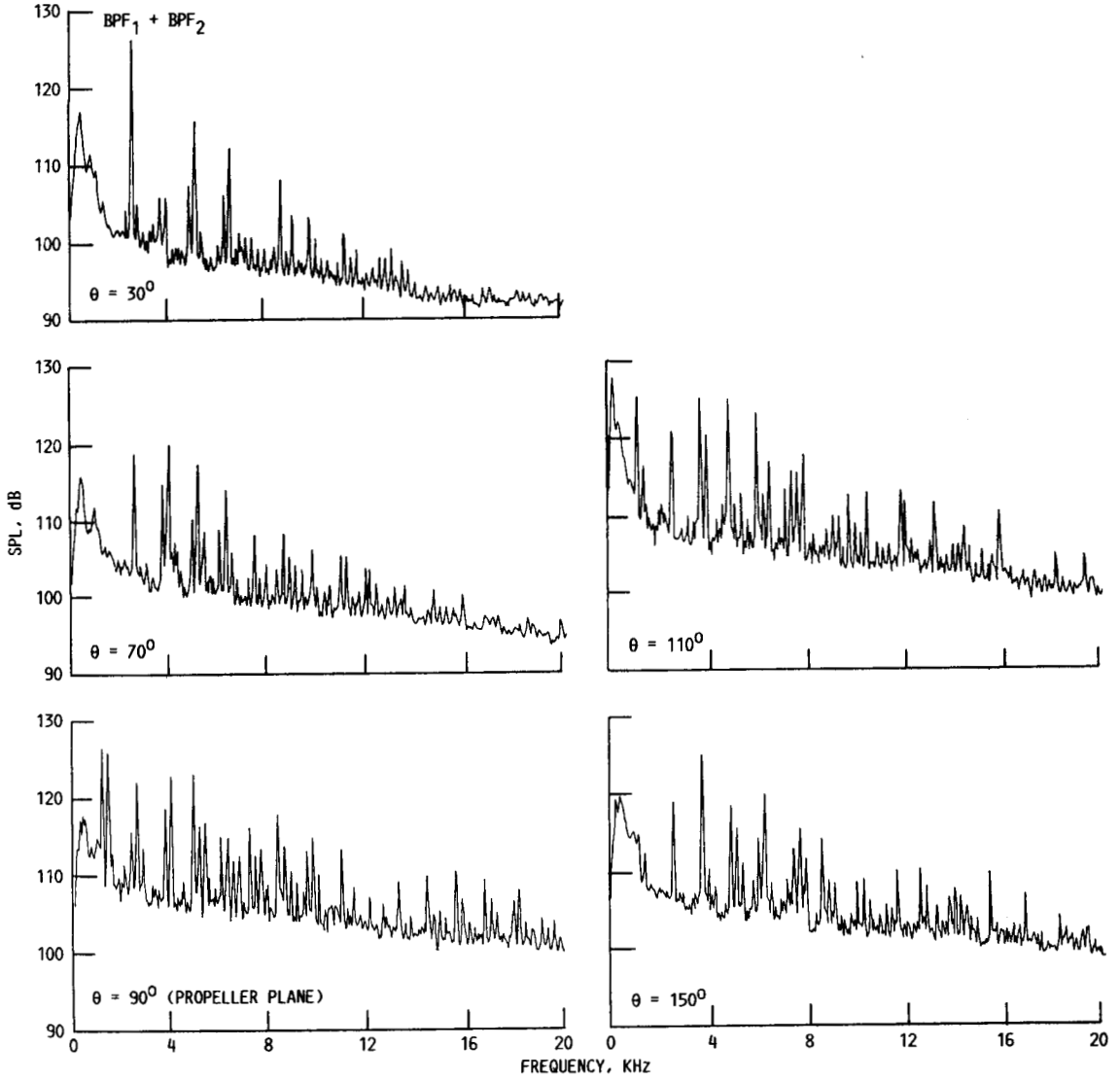

FIGURE 5. - SPL SPECTRA AT SEVERAL SIDELINE POSITIONS FOR THE F7/A7 11x9 TURBOPROP. DATA ARE FOR THE FIXED FLOOR-MOUNTED MICROPHONES. (90 PERCENT SPD, $\alpha = 0^{o}$, $B = 36.4^{o}/36.5^{o}$, NOMINAL BLADE SPACING.)

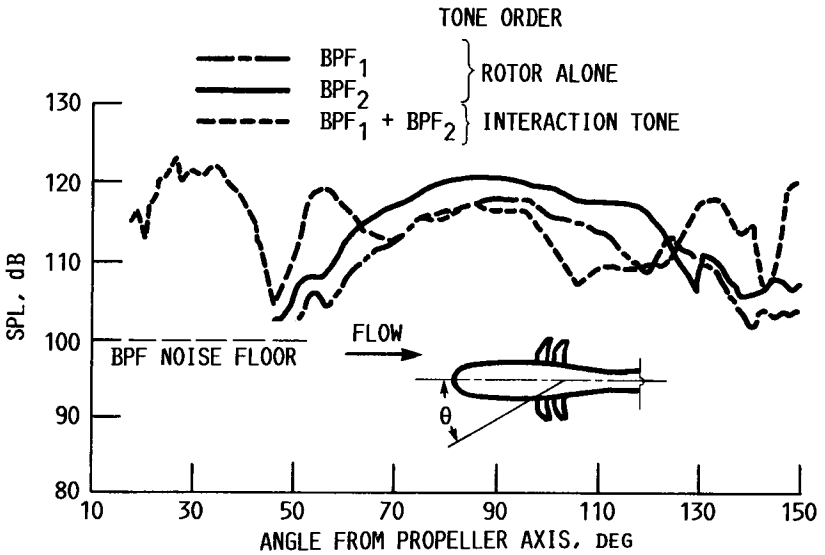

FIGURE 6. - TONE DIRECTIVITY ALONG A 137-CM (54-IN.) SIDELINE. (90 PERCENT SPD, NOMINAL SPACING, B_1/B_2 - 36.4°/36.5°, $\alpha = 0°$. 90° IS AFT PROPELLER PLANE.)

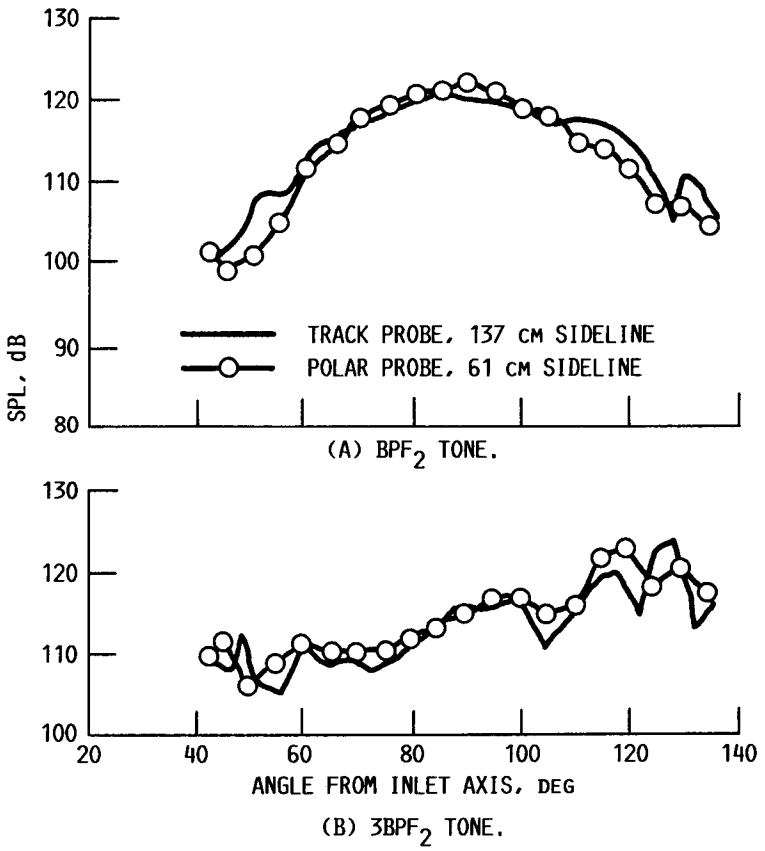

FIGURE 7. - COMPARISON OF SIDELINE DIRECTIVITY FOR POLAR AND TRACK PROBES. (DATA ADJUSTER FOR 132-CM (54-IN.) SIDELINE, 90 PERCENT SPD, $\alpha = 0°$, $B_1/B_2 = 36.4°/36.5°$, NOMINAL SPACING.)

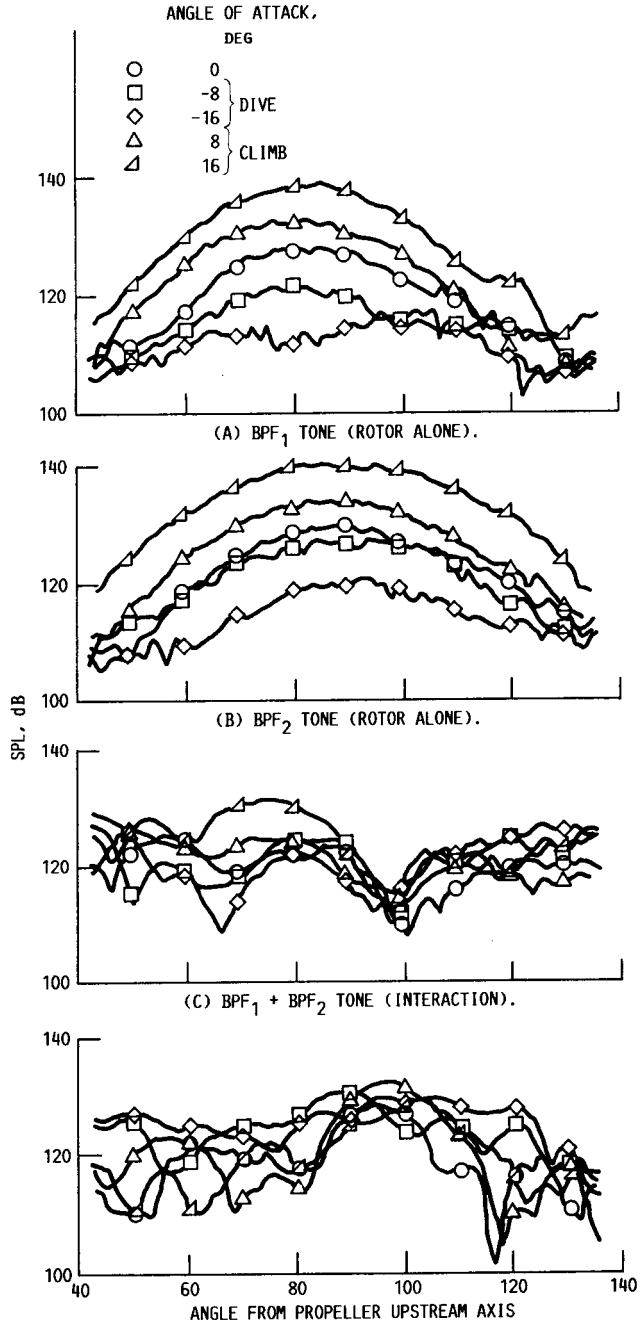

FIGURE 8. - TONE DIRECTIVITY ALONG A 61-cm (24-in.) SIDELINE FOR SEVERAL PROPELLER AXIS ANGLES OF ATTACK. (90 PERCENT SPD, $B_1/B_2 = 36.4^{\circ}/36.5^{\circ}$, NOMINAL SPACING, $M_{\infty} = 0.2$. CENTERED ON AFT PROPELLER PLANE.)

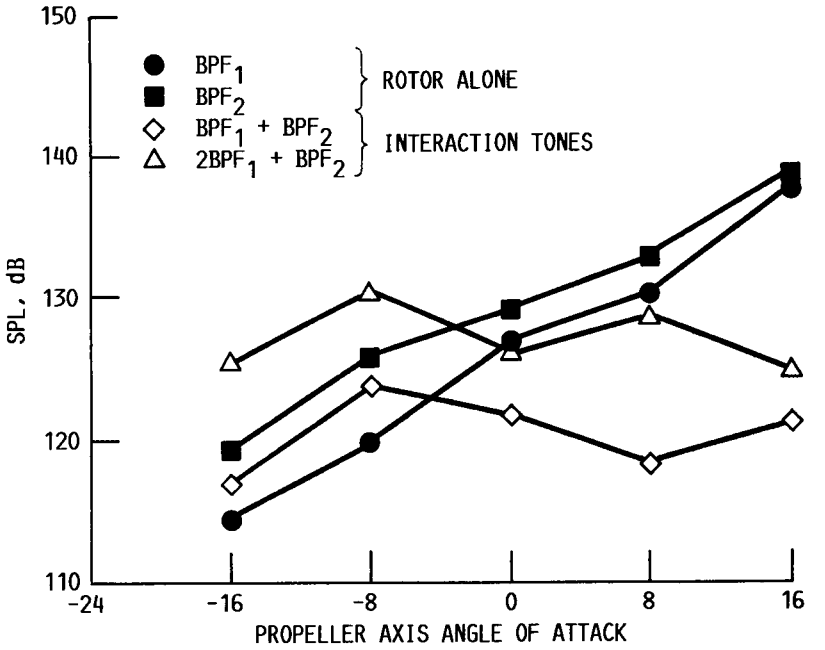

FIGURE 9. - SPL IN THE AFT PROPELLER PLANE BELOW THE AIRCRAFT, 180^{0} (90 PERCENT SPD, $B_1/B_2 = 36.4^{0}/36.5^{0}$).

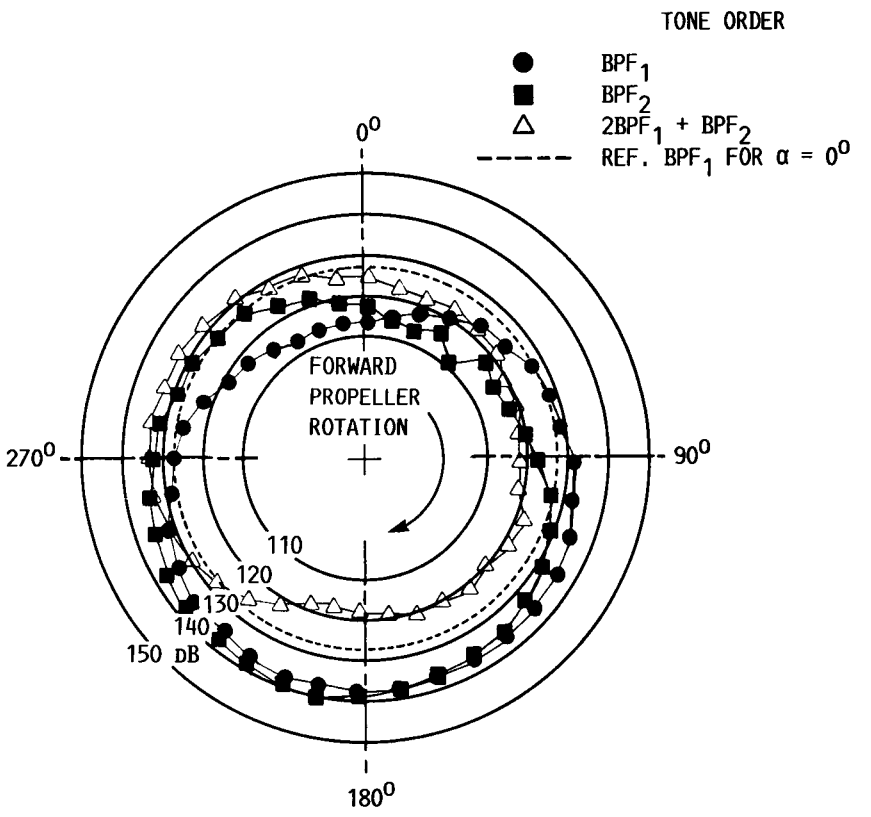

FIGURE 10. - CIRCUMFERENTIAL TONE DIRECTIVITY AT THE AFT PROPELLER PLANE FOR $\alpha = 16^{0}$. (90 PERCENT SPD, $B_1 = 36.4^{0}/36.5^{0}$, NOMINAL SPACING, $M_\infty = 0.2$.)

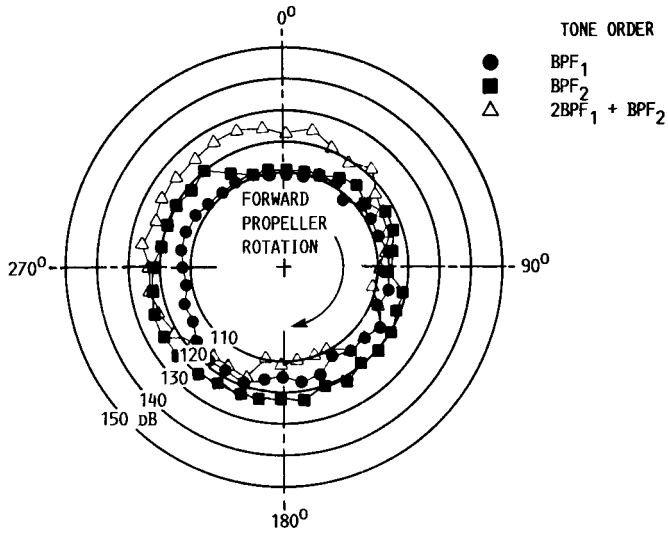

(A) 124° FROM INLET AXIS RELATIVE TO AFT PROPELLER PLANE.

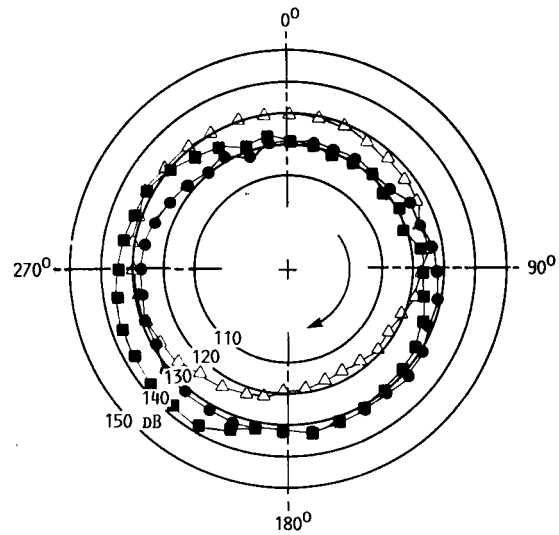

(B) AFT ROTOR PLANE.

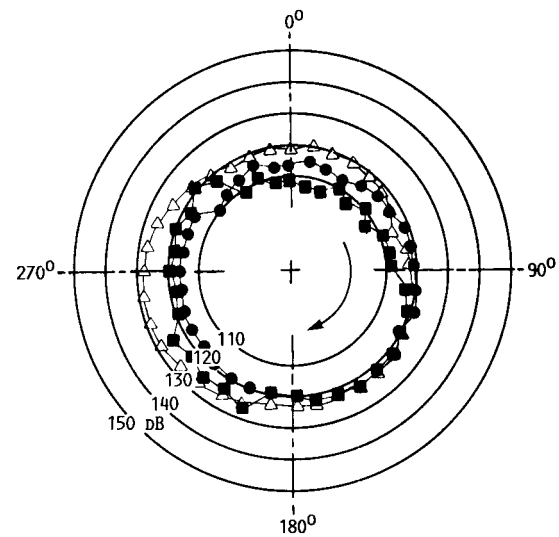

FIGURE 11. - CIRCUMFERENTIAL TONE DIRECTIVITY FOR $\alpha = 8^{\circ}$. (90 PERCENT SPD, $B_1/B_2 = 36.4^{\circ}/36.5^{\circ}$, NOMINAL SPACING, $M_{\infty} = 0.2$.)

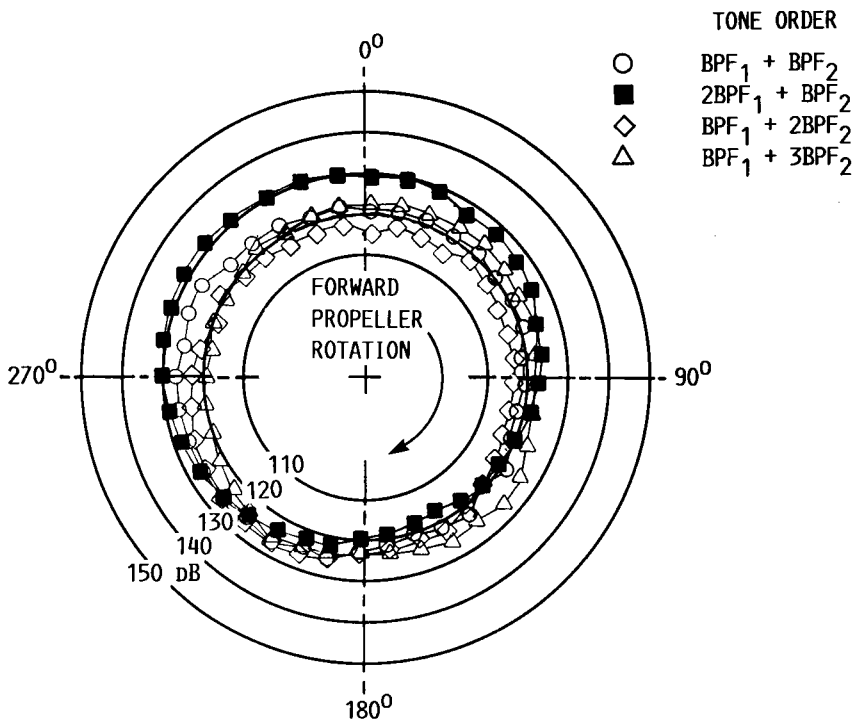

(A) AFT PROPELLER PLANE.

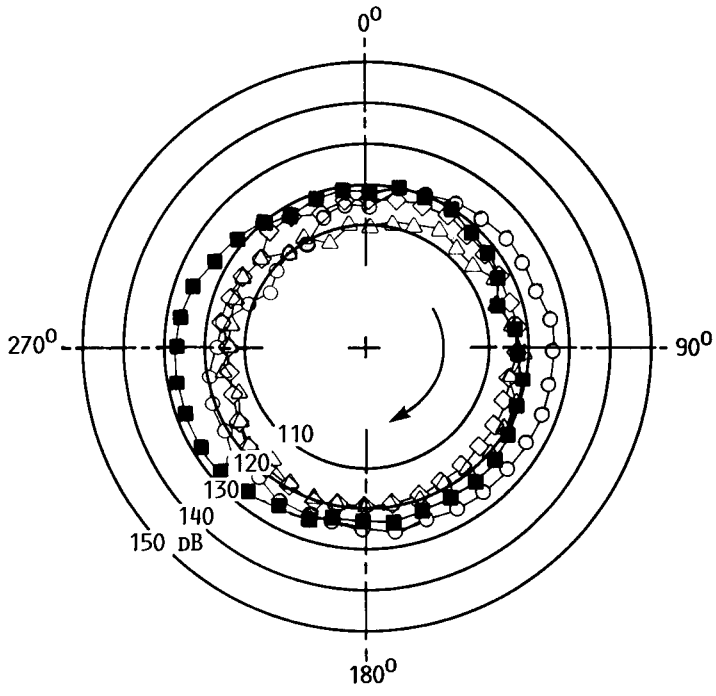

(B) 60^0 FROM PROPELLER INLET AXIS RELATIVE TO AFT PROPELLER PLANE.

FIGURE 12. - CIRCUMFERENTIAL INTERACTION TONE DIRECTIVITY FOR $\alpha = 8^0$. (90 PERCENT SPD, $M_\infty = 0.2$.)

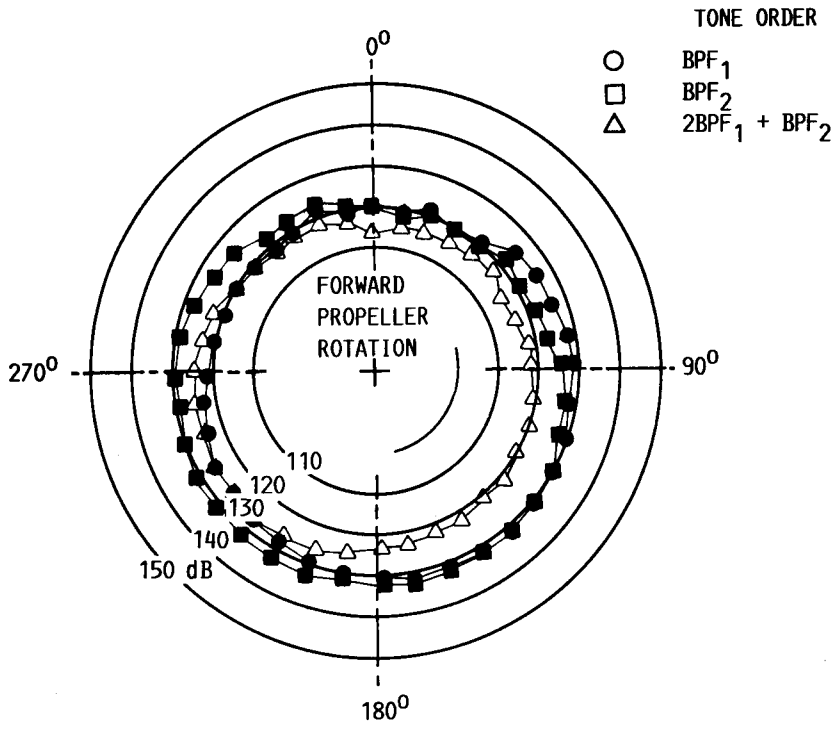

FIGURE 13. - CIRCUMFERENTIAL TONE DIRECTIVITY AT THE AFT PROPELLER PLANE FOR $\alpha = 8^0$ (90 PERCENT SPD, $B_1/B_2 = 36.4^0/36.5$, MAXIMUM SPACING).

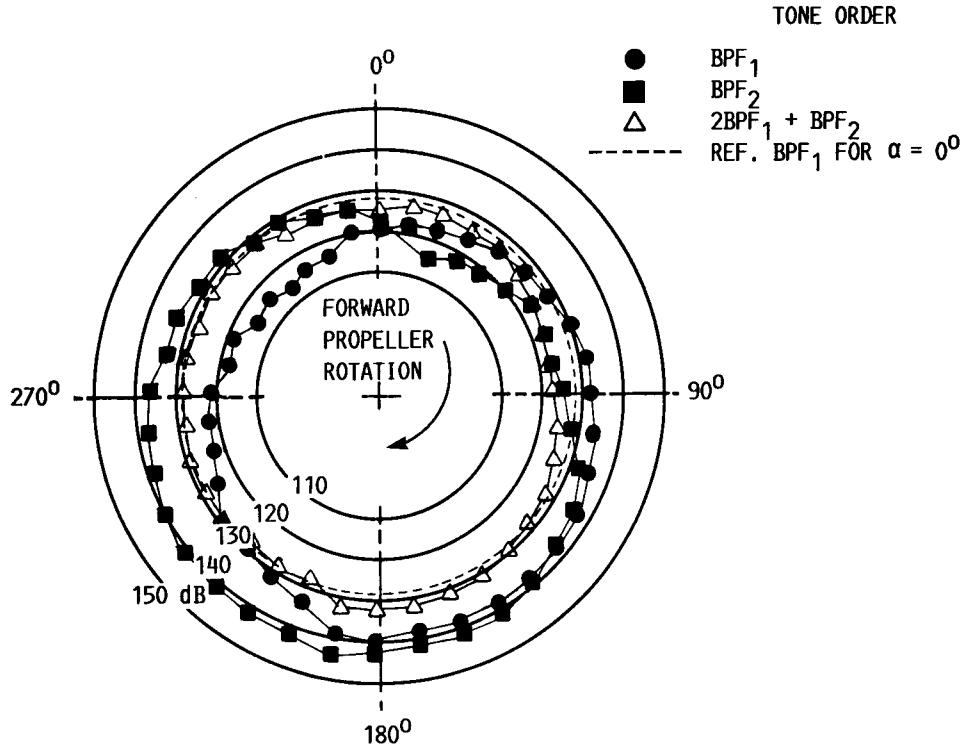

FIGURE 14. - CIRCUMFERENTIAL TONE DIRECTIVITY AT THE AFT PROPELLER PLANE FOR $\alpha = 16^0$ (90 PERCENT SPD, $B_1/B_2 = 41.1^0/39.4^0$, MAXIMUM SPACING).

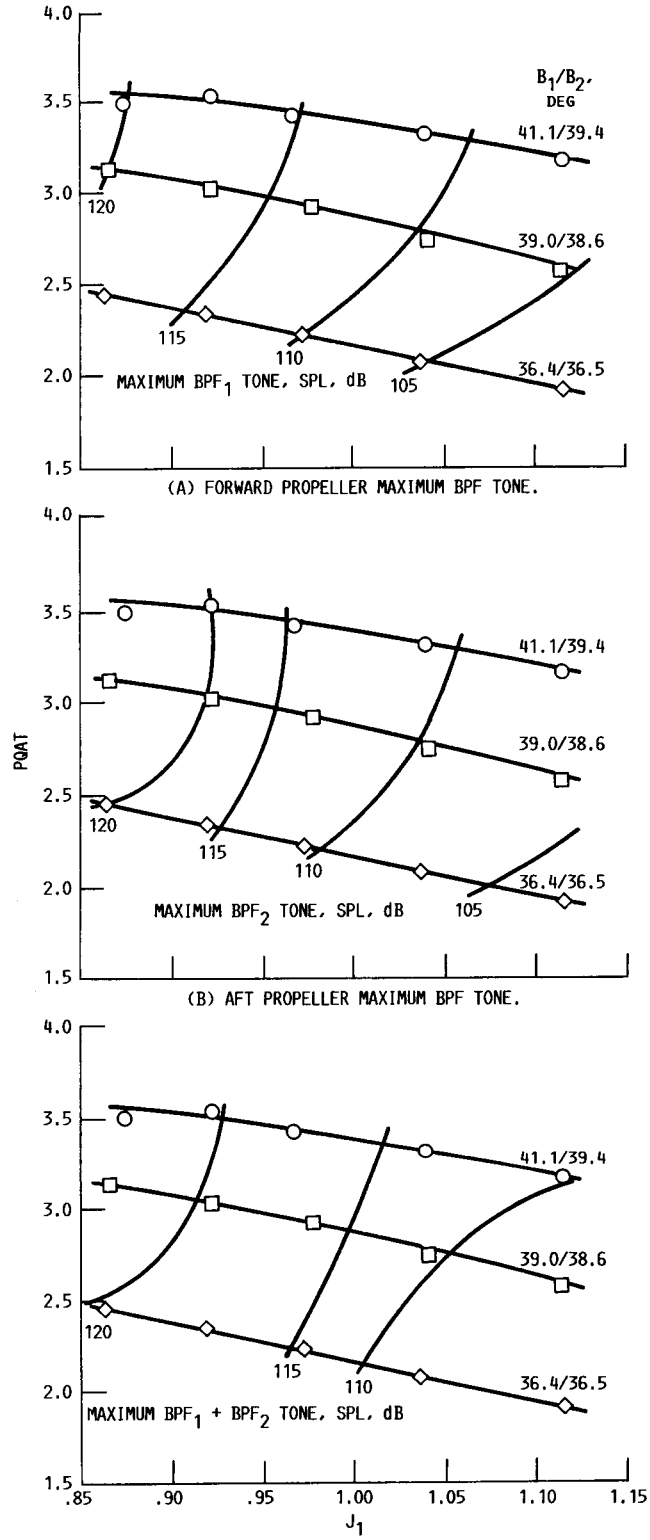

(A) FORWARD PROPELLER MAXIMUM BPF TONE.

(B) AFT PROPELLER MAXIMUM BPF TONE.

(C) MAXIMUM BPF_1 + BPF_2 INTERACTION TONE.

FIGURE 15. - MAXIMUM TONE LEVELS ALONG A 137-cm (54-in.) SIDELINE SUPERIMPOSED ON THE PROPELLER OPERTING MAP ($\alpha = 0^0$, $M_\infty = 0.2$, MAXIMUM BLADE SPACING).

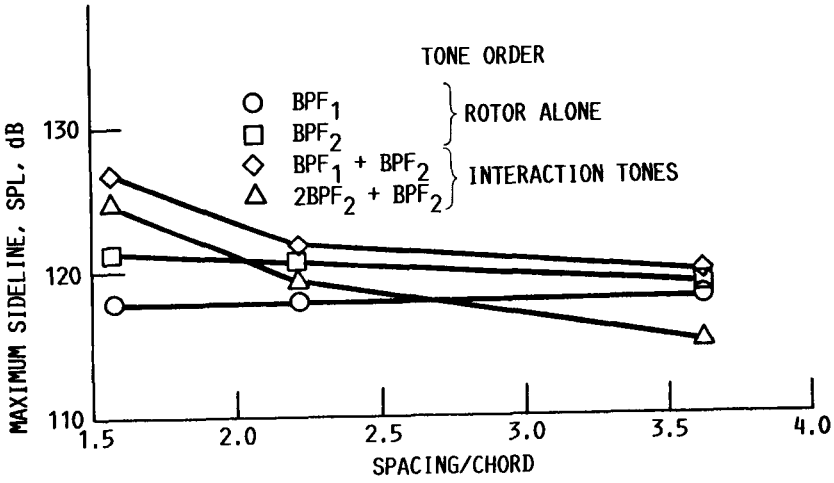

FIGURE 16. - EFFECT OF PROPELLER BLADE ROW SPACING ON MAXIMUM TONE LEVELS ALONG A 137-CM (54-IN.) SIDELINE. (90 PERCENT SPD, $B_1/B_2 = 36.4^0/36.5^0$, $\alpha = 0^0$.)

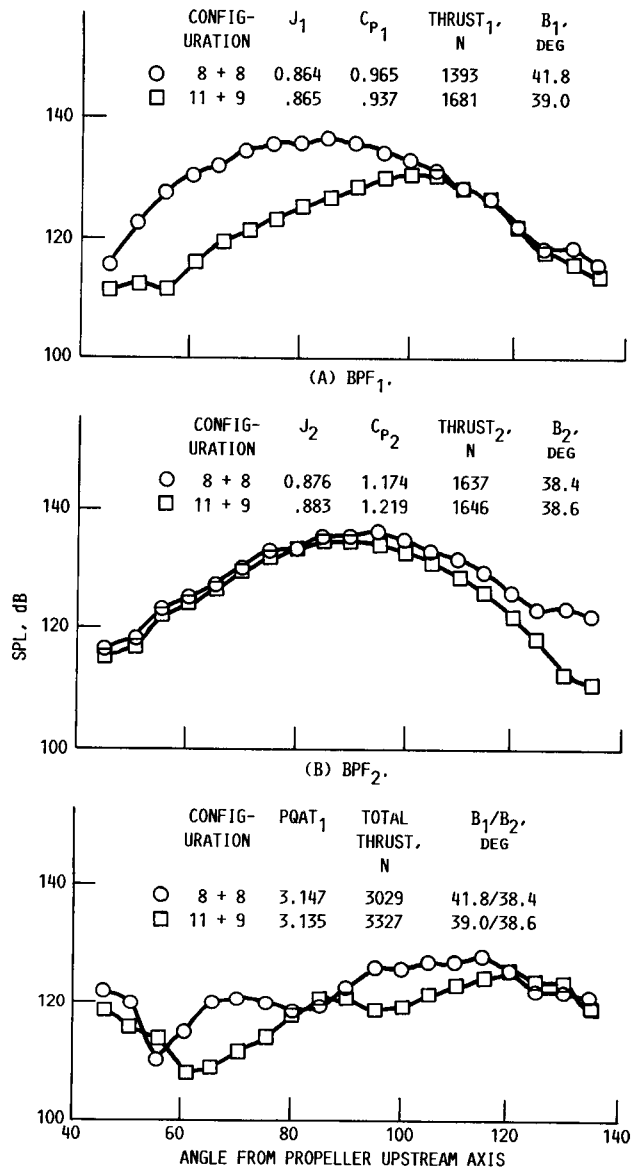

FIGURE 17. - COMPARISON OF TONE NOISE ALONG A 61-CM (24-IN.) SIDELINE FOR THE 8 + 8 AND 11 + 9 CONFIGURATIONS. (90 PERCENT SPD, RPM_1/RPM_2 = 7650/7750, M_∞ = 0.2. CENTERED ON AFT PROPELLER PLANE.)

NASA
National Aeronautics and Space Administration

Report Documentation Page

1. Report No.	2. Government Accession No.	3. Recipient's Catalog No.
NASA TM-100206 AIAA-87-2657		

4. Title and Subtitle	5. Report Date
Noise of a Model High Speed Counterrotation Propeller at Simulated Takeoff/Approach Conditions (F7/A7)	6. Performing Organization Code

7. Author(s)	8. Performing Organization Report No.
Richard P. Woodward	E-3766
	10. Work Unit No. 535-03-01

9. Performing Organization Name and Address	11. Contract or Grant No.
National Aeronautics and Space Administration Lewis Research Center Cleveland, Ohio 44135-3191	13. Type of Report and Period Covered Technical Memorandum
12. Sponsoring Agency Name and Address	14. Sponsoring Agency Code
National Aeronautics and Space Administration Washington, D.C. 20546-0001	

15. Supplementary Notes

Prepared for the 11th Aeroacoustics Conference sponsored by the American Institute of Aeronautics and Astronautics, Sunnyvale, California, October 19-21, 1987.

16. Abstract

A model high-speed advanced counterrotation propeller, F7/A7, was tested in the NASA Lewis Research Center's 9- by 15-Foot Anechoic Wind Tunnel at simulated takeoff/approach conditions of 0.2 Mach number. Acoustic measurements were taken with fixed floor microphones, an axially translating microphone probe, and with a "polar" microphone probe which was fixed to the propeller nacelle and could take both sideline and circumferential acoustic surveys. Aerodynamic measurements were also made to establish the propeller operating conditions. The propeller was run over a range of blade setting angles (front angle/rear angle) from 36.4°/36.5° to 41.1°/39.4°, tip speeds from 165 to 259 m/sec (540 to 850 ft/sec), rotor spacings from 1.56 to 3.63 based on forward rotor tip chord to aerodynamic separation, and angles of attack to ±16°. First order rotor alone tones showed highest directivity levels near the propeller plane, while interaction tones showed high levels throughout sideline directivity - especially toward the propeller rotation axis. Interaction tone levels were sensitive to propeller row spacing while rotor alone tones showed little spacing effect. There is a decreased noise level associated with higher propeller blade numbers for the same overall propeller thrust.

17. Key Words (Suggested by Author(s))	18. Distribution Statement
Turboprop Counterrotation Acoustics	Unclassified - Unlimited Subject Category 71

19. Security Classif. (of this report)	20. Security Classif. (of this page)	21. No of pages	22. Price*
Unclassified	Unclassified	24	A02

NASA FORM 1626 OCT 86

*For sale by the National Technical Information Service, Springfield, Virginia 22161